Turkish Online Journal of Qualitative Inquiry (TOJQI)
Volume 12, Issue 3, July 2021: 5322-5330

Research Article

# DEVELOPMENT OF OPTICAL PARAMETER CALCULATIONS OF THE PROBES IN WATER

Dr. Ved Nath Jha* Dr.Ghanshyam Kumar Singh**

## Abstract

Fiber optic technology with the role of surface plasmons has tremendously advanced the sensing technique of various physical, chemical and biochemical parameters of materials. The working of the optical fiber sensor designed by us is founded on the principle of the absorption of the evanescent waves passing through the optical fiber. The technique is based on the evanescent wave penetration between two dielectric media satisfying the conditions of attenuated total internal reflections (ATR's). In the present work, the cladding of the fiber is removed by a suitable technique, and Silver nanoparticles are deposited on it. The evanescent light waves passing out of the core of the fiber are absorbed by the metal nanoparticles. The wavelength of maximum absorption is specific to the metal nanoparticles as well as to the dielectric constant of the surrounding medium and occurs when the wavelength of evanescent light resonates with localized surface plasmon (LSP) wavelength of the nanoparticle. Noble metal nanoparticles of Silver and Gold exhibit LSP resonance in the visible region of electromagnetic spectrum. In this article, we report the characteristic parameters of three sensor probes a, b and c developed by researcher.

***Keywords:*** Optical, Fiber, Metal, Probes etc.

## 1. INTRODUCTION

Optical fibers is commonly used in all fields of industry because of their superior characteristics compared to traditional data transmission systems they are used in the field of telecommunications. Dr. K. C. Kao and his colleagues at standard telecommunications laboratories Ltd developed the principle of guiding light with optical fibers. Optical fibers networking is free of electromagnetic interference as well as of interference from microwaves and radiofrequency and enables multiple light waves to be simultaneously transmitted through one single fiber. The materials that are used to produce optical fibers are dielectric, immunized against electric conductivity and thus ensure greater protection.

At the same time, researchers are fascinated that their peculiar characteristics make them highly attractive for sensing applications. Optical fibers have acquired a large range of sensor systems for accurate detection and analysis of various contaminants.

[1] Department of Physics, Mangalayatan University, Aligarh, (Uttar Pradesh)
[2] Department of Physics, Himalayan University, Ita Nagar (Arunachal Pradesh)

## 2. THEORETICAL BACKGROUND OF THE STUDY

The optical source considered is an un-polarized collimated beam. The evanescent field of the propagating rays interacts with the metal nanoparticles coated on an unclad region of the fiber and excites surface plasmon modes. A strong absorption band is observed when the surface plasmon wavelength matches with the wavelength of the evanescent field. The localized surface plasmon wavelength depends on the type, size, and shape of the nanoparticles as well as the dielectric constant of the surrounding medium. The absorption from a single metal nanoparticle is related to its real and imaginary part of the dielectric constant $_1(\lambda, R)$ as given by

$$Re(\epsilon_1(\lambda, R)) = \epsilon^{\infty} - \frac{\lambda^2\lambda_c^2}{\lambda_p^2(\lambda_c^2 + \lambda^2)} \quad (1)$$

And

$$Im(\epsilon_1(\lambda, R)) = \frac{\lambda^3\lambda_c}{\lambda_p^2(\lambda_c^2 + \lambda^2)}. \quad (2)$$

The above expressions were reported within the framework of the Drude model. $\lambda_p$ and $\lambda_c$ are the plasma wavelength and collision wavelength, respectively, of the nanoparticle which is specific to a given sensor and $^{\infty}$is the high-frequency dielectric constant which occurred due to interband transitions. The value of $^{\infty}$ for Silver lies between 4.7 − 5.3. In our case, we have taken $^{\infty}$ = 5.13 for the calculation of optical parameters of prepared fiber optic sensor probes.

In the case of evanescent wave absorption in optical fibers, one needs to take into account the absorption coefficient of the ray making an angle $\theta$ with the normal to the interface and other parameters characteristic of the metal nanoparticles deposited on the core of the fiber as well as the length of the sensing region. Gupta et al., have obtained the evanescent absorption coefficient for spherical metallic nanoparticles deposited on optical fiber core as

$$\gamma(\theta, \lambda) = \frac{NE\lambda n_2 cos\theta cot\theta}{2\pi\rho L n_1^2 cos\alpha cos^2\theta_c (sin^2\theta - sin^2\theta_c)^{1/2}}. \quad (3)$$

Here, E is the extinction (scattering + absorption) of a single metal nanoparticle, $\alpha$ is the skewness parameter for the rays having values between 0 to $\pi/2$. $\theta_c$ is the critical angle of the sensing region, $\lambda$ is the wavelength of light used and $\theta$ is the angle that the incident ray makes with the normal to the interface. $n_1$, $n_2$ are the refractive indices of the optical fiber core and metal nanoparticle, respectively. N is the total number of nanoparticles attached to the bare core of the fiber given by

$$N = \frac{2\pi\rho L}{4R^2}. \quad (4)$$

ρ and R being the radii of the core and the metal nanoparticle, respectively and L is the length of the sensing region. The extinction of a single metal nanoparticle is given by

$$E = \frac{24\pi R\epsilon_m^{3/2}}{\lambda} \frac{Im(\epsilon_1(\lambda, R))}{[Re(\epsilon_1(\lambda, R)) + 2\epsilon_m)^2 + Im(\epsilon_1(\lambda, R))^2]}. \quad (5)$$

Here, $_m$ is the dielectric constant of the surrounding medium. One can notice that the condition for maximum extinction occurs when

$$Re(\epsilon_1(\lambda, R)) = -2\epsilon_m. \quad (6)$$

This condition is specific to the intrinsic parameters $\lambda_p$, $\lambda_c$ of the sensing region. Under the practical situation, the number of deposited nanoparticles, as well as the size uniformity of the nanoparticles on the fiber core cannot be ensured. However, a rough estimate of the intrinsic parameters for a given sensor probe immersed in a medium of known dielectric constant can be obtained from the experimentally measured transmitted output power at different wavelengths. The output power P from the sensor probe can be related to the launched power $P_0$ via the relation

$$P = P_0 \exp(-\gamma(\theta, \lambda)L). \quad (7)$$

Here, L is the length of the sensing region and $\gamma(\theta, \lambda)$ is the evanescent absorption coefficient of the sensing medium given by equation (3).

## 3. RESULTS & DISCUSSION

The theoretical analysis described above suggest that the sensor probe can be characterised by its plasma and collision wavelength. We have obtained these parameters for the probes a, b and c using the experimental results obtained for the surrounding media of known dielectric constant Viz; water and air. The characteristic wavelengths $\lambda_p$, $\lambda_c$ of the three sensor probes a, b and c are obtained from the experimental observations reported in which air and distilled water are the surrounding media of which the dielectric constants are taken as the standard values 1 and 1.768, respectively by assuming them to be nondispersive. The wavelength of maximum extinction for air ($\lambda_a$) and water ($\lambda_w$) have been obtained experimentally. The straightforward calculations of the plasmon wavelength ($\lambda_p$) and the collision wavelength ($\lambda_c$) as the functions of the maximum extinction wavelength are obtained by making use of equations (1) and (6) which yields

$$\lambda_p^2 = \frac{1.5\lambda_a^2\lambda_w^2}{61.55\lambda_w^2 - 61.81\lambda_a^2}; \quad (8)$$

And

$$\lambda_c^2 = \frac{1.5\lambda_a^2\lambda_w^2}{7.13\lambda_w^2 - 8.67\lambda_a^2}. \quad (9)$$

Making use of equations (8) and (9), the values of plasma wavelength and collision wave-length for the probes a, b and c were obtained as shown in table 1.

**Table 1: Experimentally obtained values of plasma wavelength ($\lambda_p$) and collision wavelength ($\lambda_c$) for the probes a, b and c.**

| S. No. | Probe | NP size (nm) | $^{\lambda}a$ (nm) | $^{\lambda}w$ (nm) | $^{\lambda}c$ ($\mu$m) | $^{\lambda}p$ (nm) |
|---|---|---|---|---|---|---|
| (i) | a | 107 | 401 | 430 | 76.7 | 176.43 |
| (ii) | b | 132 | 406 | 433 | 74.9 | 185.51 |
| (iii) | c | 140 | 410 | 434 | 64.2 | 185.93 |

The substantial variation in the collision wavelength ($\lambda_c$) and minor changes in plasmon wave-length ($\lambda_p$) with increasing nanoparticle size can be viewed from table 1. The values of $\lambda_c$ and $\lambda_p$ indicate that the collision wavelength decreases with increasing nanoparticle size while the plasmon wavelength appears to be nearly independent of it. In general, the collision wavelength is expected to increase with the increase in nanoparticle size contrary to our observations. The discrepancy of our results might be due to large nanoparticle size variation as well as non-uniform deposition of the nanoparticles on the unclad region of the optical fiber. However, in the table 3.1, the average size of the nanoparticles are given. The above observation also suggests that the SPR wavelength decreases with increasing collision wavelength.

We have theoretically estimated SPR wavelength for four different situations, where the dielectric constant of the surrounding medium are chosen as $_m$ = 1.4, 1.7, 2.0 and 2.3 and the values of plasma wavelength ($\lambda_p$) and collision wavelength ($\lambda_c$) are taken from table 1. Figure (1) shows the variation of dielectric constant of metal nanoparticle $Re(\ _1(\lambda, R))$ as given by equation (1) with respect to the wavelength of light ($\lambda$), for the probes a, b and c. Straight lines in the figure correspond to twice the dielectric constant of the surrounding medium ($2\ _m$) taken for analysis. The intersection of the curves of $Re(\ _1(\lambda, R))$ and $2\ _m$ represent the SPR wave-length. Figure (1) clearly shows that SPR wavelength decreases with increasing dielectric constant of the surrounding medium. Since we are focusing our attention on the working of the fiber sensor in the visible region, figure 1 clearly indicates that the applicability of the sensor is limited to the dielectric constant of the surrounding media between 1.4 and 2.0 only.

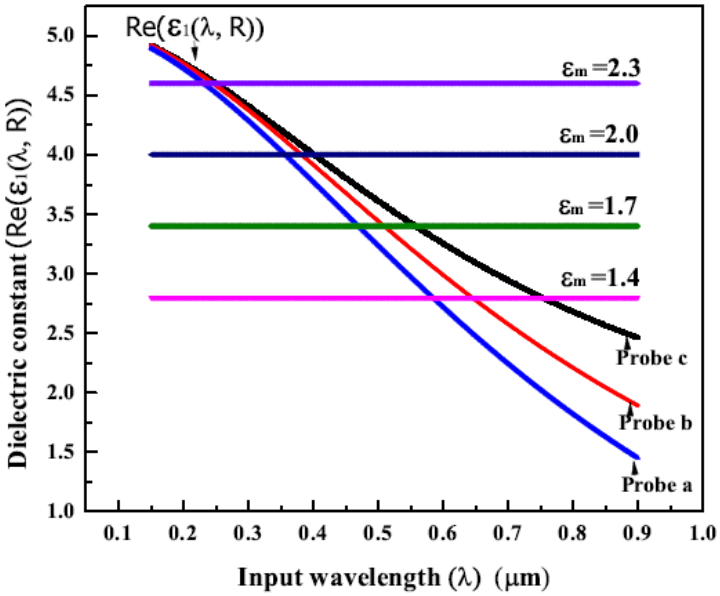


**Figure 1: Variation of dielectric constant of metal nanoparticle (*Re*( $_1$(*λ*, *R*))) with respect to wavelength of light (*λ*).**

We had also examined the output intensity when the dielectric constant of the surrounding media was $_m$ = 1.4, 1.7 and 2.0 for the probes a, b and c. Figures 2 to 4 exhibit a dip in the output intensity at the SPR wavelength which decreases with the increase in the dielectric constant of the surrounding medium. The sensor probe performance appears to improve with increasing dielectric constant of the surrounding medium as evident from the maximum extinction shown in figure 4.

In the practical situations, impurities of various dielectric constant are simultaneously present in water. We extend the above theoretical model for such situation and define the output power

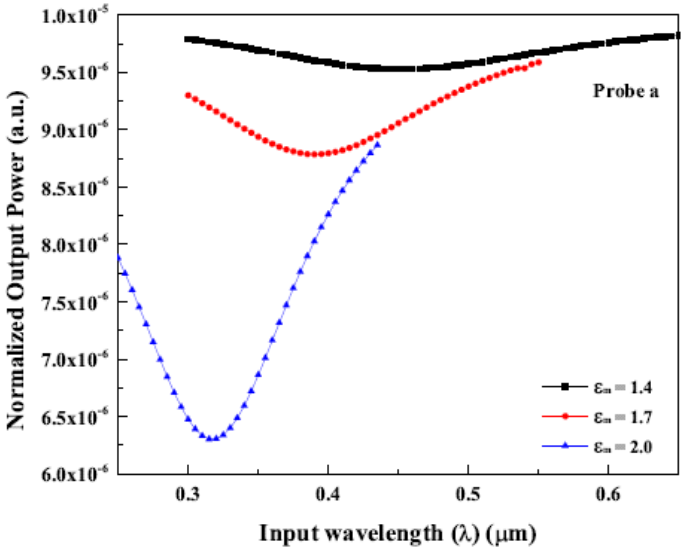

**Figure 2: Wavelength ($\lambda$) versus normalized output power for medium of different dielectric constant ( $_m$) for probe a.**

as

$$P = P_0[exp(-\gamma_1 L) + exp(-\gamma_2 L) + exp(-\gamma_3 L) + ...]. \quad (10)$$

Here $P_0$ is the launched input power, $\gamma_i$ is effective evanescent absorption coefficient of the components of the impurities. It is worthy to mention that the dielectric constant of the solution surrounding the fiber sensor changes with the change in the solute concentration.

We have plotted the wavelength versus output power for sensor probes a, b and c, when the surrounding medium is taken as the mixture of components of given dielectric constant 1.4, 1.7, and 2.0. Figures 5 to 7 exhibit the distinct LSP resonance dips corresponding to the different component of the known dielectric constant present in the mixture. The theoretical results are tested in case of simultaneous detection of impurities in water.

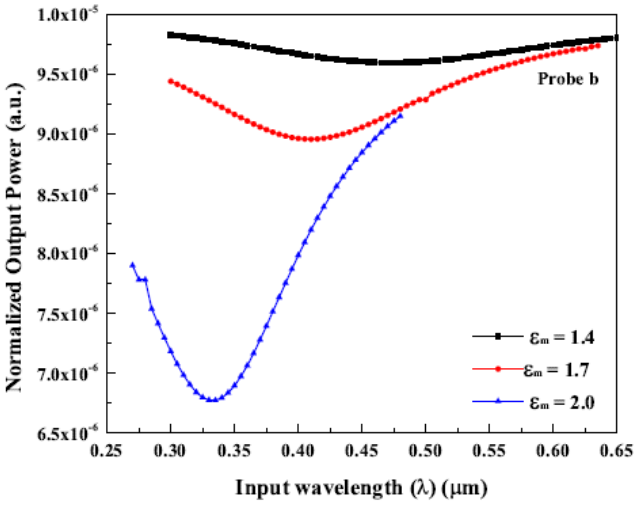


**Figure 3: Wavelength ($\lambda$) versus normalized output power for medium of different dielectric constant ( $_m$) for probe b.**

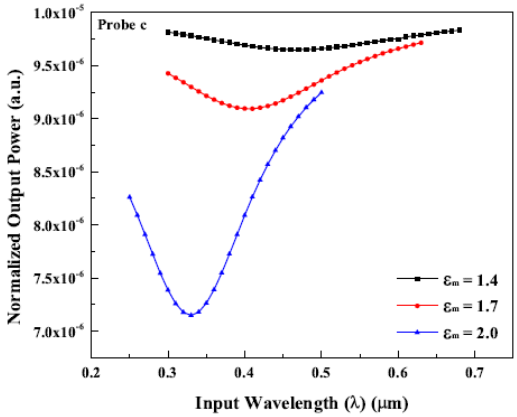

**Figure 4: Wavelength ($\lambda$) versus normalized output power for medium of different dielectric constant ( $_m$) for probe c.**

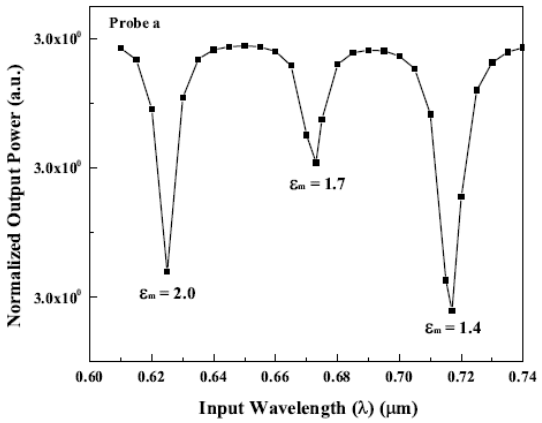


**Figure 5: Wavelength ($\lambda$) versus normalized output power for medium of different dielectric constant taken simultaneously ( $_m$ = 1.4, 1.7, and 2.0) for probe a.**

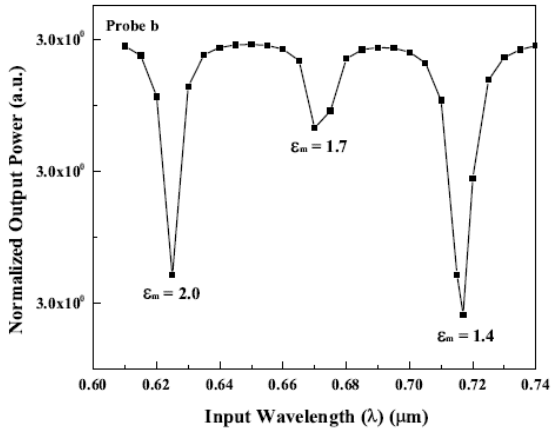


**Figure 6: Wavelength ($\lambda$) versus normalized output power for medium of different dielectric constant taken simultaneously ( $_m$ = 1.4, 1.7, and 2.0) for probe b.**

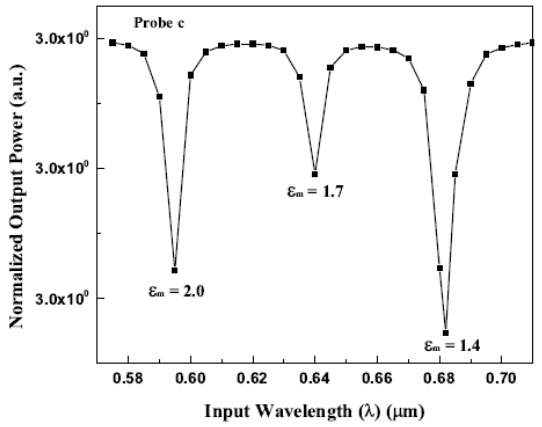

**Figure 7: Wavelength ($\lambda$) versus normalized output power for medium of different dielectric constant taken simultaneously ( $_m$ = 1.4, 1.7, and 2.0) for probe c.**

## 4. CONCLUSION

Precise measurement of toxic impurities in water is of significant importance in light of human health. In general, water is highly contaminated and includes different kinds of contaminants near fertiliser plants and the industry. The article focused on experimental activities to detect impurities in fluorides, chromium and arsenic using a fibre optic filter sensor in potable water. The principle of working of the fabricated fiber optic sensor probe is localized surface plasmon resonance (LSPR). The plasmon resonance induced in the metal nanoparticles under the influence of an electromagnetic wave of frequency same as the frequency of oscillation of electron cloud in metal nanoparticles enhances the absorption. We have deposited Silver nanoparticles on a part of the unclad region of the optical fiber using a laser-induced nanoparticle deposition technique. This technique of the deposition of the Silver nanoparticle is very simple and quick. The Silver based sensor is known for its narrow spectral width and the high detection accuracy. Although, Silver is chemically unstable and is highly vulnerable to oxidation. Silver nanoparticles are sensitive towards the impurity which inspired us to choose Silver nanoparticles for the deposition to make the sensor probe.

## REFERENCES

[1]. N. George, A. M. Paul, and M. S. Saranya, 'Microbend fiber optic detection of continuously varying refractive index of chlorinated water', Optik - International Journal for Light and Electron Optics, vol. 125, no. 1, pp. 301– 303, Jan. 2014.
[2]. M. Afzal, 'Introduction to fibre-optic sensing system and practical applications in water quality management', 2013 Fourth International Conference on Computing, Communications and Networking Technologies (ICCCNT), Jan. 2013.
[3]. M. Li, D. Li, Q. Ding, Y. Chen, and C. Ge, 'A Multi-parameter Integrated Water Quality Sensors System', IFIP Advances in Information and Communication Technology, pp. 260–270, Jan. 2013
[4]. Wencel, B. D. MacCraith, and McDonagh, 'High performance optical ratiometric sol–gel-based pH sensor', Sensors and Actuators B: Chemical, vol. 139, no. 1, pp. 208–213, Jan. 2009.
[5]. J.-H. Pai, D. Davey, and H.-Y. Hsu, 'Essential elements of biosensor development for water quality monitoring', 2011 Seventh International Conference on Intelligent Sensors, Sensor Networks and Information Processing, Jan. 2011.
[6]. Sohanghpurwala, Aliasgar, Govind Rao, and Yordan Kostov. "Optical replacement of pH electrode." Sensors Journal, IEEE 9.3 (2009): 219-220.
[7]. Z. Dong, U. Wejinya, J. Vaughan, and A. Albrecht, 'Fabrication and testing of ISFET based pH sensor for microliter scale solution targets', 2012 IEEE Nanotechnology Materials and Devices Conference (NMDC2012), Jan. 2012.
[8]. N. George, A. M. Paul, and M. S. Saranya, 'Microbend fiber optic detection of continuously varying refractive index of chlorinated water', Optik - International Journal for Light and Electron Optics, vol. 125, no. 1, pp. 301– 303, Jan. 2014.

[9]. L. Zhang and X. Gu, 'Study on residual chlorine detecting system based on dual-wavelength optical path', 2010 International Conference on Computer Application and System Modeling (ICCASM 2010), Jan. 2010.

[10]. Daniyal, W.M.E.M.M.; Saleviter, S.; Fen, Y.W. Development of Surface Plasmon Resonance Spectroscopy for Metal Ion Detection. *Sens. Mater*. **2018**, *30*, 2023–2038.

[11]. Liu, X.; Yao, Y.; Ying, Y.; Ping, J. Recent advances in nanomaterial-enabled screen-printed electrochemical sensors for heavy metal detection. *Trends Anal. Chem.* **2019**, *115*, 187–202

[12]. Raj, D.R.; Prasanth, S.; Vineeshkumar, T.V.; Sudarsanakumar, C. Surface Plasmon Resonance based fiber optic sensor for mercury detection using gold nanoparticles PVA hybrid. *Opt. Commun.* **2016**, *367*, 102–107.